의학박사 학위논문

암세포 유래 exosome이 RCAN1.4 조절을 통해 암세포의 성장에 미치는 영향

Tumor-derived exosomes promote tumor growth through the modulation of RCAN1.4

울산대학교대학원

의학과

박소정

Tumor-derived exosomes promote tumor growth through the modulation of RCAN1.4

지도교수 최창민

이 논문을 의학박사학위 논문으로 제출함

2018년 12월

울산대학교대학원

의학과

박소정

박소정의 의학박사학위 논문을 인준함

심사위원 이재철 인

심사위원 최창민 인

심사위원 김형렬 인

심사위원 노진경 인

심사위원 박찬권 인

울산대학교대학원

2018년 12월

감사의 글

호흡기내과 의사라는 명칭으로 자기 소개를 하게 된 것이 이제 4년째입니다. 아직 모르는 것이 많지만 계속 배우고 싶다는 생각이 들게 하는 재미있고 매력적인 학문이 호흡기학이라고 생각합니다. 제가 박사 학위 논문을 무사히 마치게 된 것은 많은 가르침과 격려를 아끼지 않으신 많은 분들의 관심과 도움이 있었기 때문입니다. 이 기회를 빌어 그 분들께 감사의 말씀을 올리고자 합니다.

지도교수님이신 최창민 교수님께서는 처음 이 연구를 수행할 수 있도록 기회를 주시고 전반적인 연구의 방향과 흐름을 파악할 수 있도록 도와주셨습니다. 제가 언제나 믿고 의지할 수 있는 든든한 선생님이 되어주셔서 감사드리며, 항상 새로운 것에 도전하고 발전해 나가시는 모습을 따라가는 제자가 되도록 노력하겠습니다. 심사위원장님이신 이재철 교수님은 제가 처음 폐암에 관심을 가질 수 있도록 이끌어 주신, 제 인생에 정말 큰 영향을 주신 분입니다. 제가 힘들어하고 방황할 때마다 따뜻한 손길로 아낌없는 가르침을 주심에 감사드리며 깊은 존경과 감사의 말씀을 올립니다. 또한 연구 과정 중에 내용 하나하나 꼼꼼하게 살펴 주시고 많은 동기 부여를 통해서 이끌어 주신 노진경 교수님과 가까이서 작은 물음 하나에도 기꺼이 도움을 주시며 기초에서부터 마지막까지 곁에서 세심한 조언을 아끼지 않으신 김동하 박사님께 감사 드립니다. 마지막으로 부족한 내용임에도 불구하고 바쁜 시간을 할애하여 기꺼이 심사 위원을 맡아주시고 논문의 내용과 방향에 대해서 조언을 아끼지 않으신 김형렬 교수님, 박찬권 교수님께 감사드립니다.

의사로서 한 발씩 걸음을 내딛을 때마다 제가 존재할 수 있도록 물심양면으로 이끌어주신 분들의 노고를 잊지 않겠습니다. 모든 분들께 감사와 사랑을 전하며, 더욱 더 정진하도록 최선을 다하겠습니다. 감사합니다.

2018년 12월

국문요약

세포 간의 의사 소통과 그 주변의 종양 미세 환경은 암세포의 성장에 매우 중요한 역할을 한다. 엑소좀은 거의 대부분의 세포에서 분비되는 것으로, 암세포에서 유래한 엑소좀은 암세포 간의 단백질이나 RNA 등의 물질을 주고 받는 매개체 역할을 함으로서 암세포의 악성도 강화와 면역 감시 회피, 신생 혈관 형성 및 항암제 저항성 등을 일으키는 것으로 알려지고 있다. 본 연구는 A549 세포주에서 유래한 엑소좀이 다른 폐암 세포주에서 유래한 엑소좀과 비교하여 혈관 내피 세포에서 신생 혈관 형성을 촉진하는지에 대하여 연구한 것이다. 본 연구에서는 A549 세포주 유래 엑소좀 내의 특정 miRNA를 miRNA array를 이용하여 찾아낸 후 이 특정 miRNA가 신생 혈관 형성을 조절하는지 알아보았다.

연구 결과, 여러가지의 후보 miRNA 중 miRNA-619-5p가 혈관 내피 세포에서 신생 혈관의 형성을 유의하게 촉진하는 것으로 확인되었다. miRNA-619-5p는 직접적으로 RCAN1.4를 타겟으로 하며, miRNA-619-5p 발현이 증가하면 RCAN1.4의 발현이 의미 있게 감소하는 것으로 확인되었다. 비소세포폐암 환자에서 획득한 조직에서 RCAN1.4의 발현 정도는 주변의 정상 폐 조직에 비하여 암 조직에서 의미 있게 감소되어 있었으며, 그와는 반대로 miRNA-619-5p의 발현 정도는 암 조직에서 의미 있게 증가되어 있었다. 또한 miRNA-619-5p와 RCAN1.4의 발현 정도는 역의 상관 관계를 가지고 있었다. 더불어, miRNA-619-5p는 정상인에 비하여 비소세포폐암 환자의 혈장에서 분리된 엑소좀에서 더 높게 측정되었고 RCAN1.4 발현 정도는 비소세포폐암 환자의 전체 생존율과도 의미 있는 관련성을 보였다.

따라서 엑소좀 내 miRNA-619-5p의 발현 정도는 비소세포폐암의 진단과 예후 예측에 사용될 수 있을 것으로 기대되며, 향후 RCAN1.4의 조절을 통한 신생 혈관 형성과 암세포의 성장 기전에 대한 보다 자세한 추가 연구가 필요하다.

Key words: Non-small cell lung cancer, angiogenesis, RCAN1.4, MicroRNAs, angiogenesis

차례

List of figures

List of abbreviations

NSCLC = non-small-cell lung cancer

RCAN1 = Human regulator of calcineurin 1

NFAT = nuclear factor of activated T-cells

FBS = fetal bovine serum

HUVECs = Human umbilical vein endothelial cells

PBS = phosphate-buffered saline

EM = electron microscope

RNA seq = RNA sequencing

Introduction

Lung cancer is the leading cause of death worldwide. More than 40% of newly diagnosed patients present with metastatic disease [1, 2]. However, clinical success of targeting the EGFR mutation or ALK rearrangement with tyrosine kinase inhibitors has shown the importance of identification of molecular subtypes of non-small-cell lung cancer (NSCLC) [3, 4]. Therefore, it is necessary to investigate the novel causative genes and molecular pathways underlying lung cancer progression and metastasis.

Cells shed small vesicles from their membrane to blood vessel and body fluids [5]. Those vesicles are described as exosomes, extracellular vesicles, shedding vesicles, microparticles, and microvesicles. These vesicles contain intracellular DNA, mRNA, miRNA, and proteins. These can adhere and fuse to circulating or distant resident cells, allowing those to deliver cytoplasmic components to distant cells [6-8]. Recently, numerous studies have been investigated the role of exosomes in intercellular communication and substance exchange between tumor cells and other cells in the tumor microenvironment. Exosomes derived from lung cancer cell are known to regulate tumor growth, angiogenesis, metastasis, drug resistance, and immune escape [9-17]. Malignant tissues are highly heterogeneous, so exosomes excreted from aggressive malignant cells could change the characteristics of nonaggressive malignant cells [18-20].

Human regulator of calcineurin 1 (RCAN1) is an endogenous protein which interacts with calcineurin and then inhibits its function by interfering with calcineurin–nuclear factor of activated T-cells (NFAT) pathway [21]. RCAN1 has been known to have a wide range of biological roles, including protecting against calcium-mediated oxidative stress, cardiac

hypertrophy, and VEGF-mediated signaling during angiogenesis [22-24]. Angiogenesis is crucial for tumor growth. Previous reports demonstrated that overexpression of RCAN1 in vascular endothelium cells contributes to generalized cancer protection by inhibiting the formation of an effective tumor vasculature via inhibition of the calcineurin pathway [25, 26]. In addition, overexpression of RCAN1 significantly attenuates the malignancy, including decreased ability of proliferation, colony formation, migration and invasion [27]. RCAN1.1 and RCAN1.4 are the two major isoforms differentially expressed in many tissues and cells. While RCAN1.1 is constitutively expressed, expression of RCAN1.4 is induced by various physiological stimuli [28]. A previous study demonstrated that RCAN1.4 mRNA and protein levels were significantly decreased in hepatocellular carcinoma compared with adjacent normal liver tissues [29]. Reduced RCAN1.4 mRNA levels were significantly associated with advanced tumor stages, poor differentiation, larger tumor size, and vascular invasion. In addition, low RCAN1.4 mRNA levels were associated with poor survival and early recurrence. Moreover, downregulation of RCAN1 resulted in enhanced invasive and migratory ability in small-cell lung cancer [30]. Increased RCAN1 level promoted lymphoma cell apoptosis and was associated with thyroid cancer growth and metastasis suppressor in vivo [31, 32].

However, the function of RCAN1.4 has only scarcely been investigated in tumor development and prognosis of NSCLC. In this study, we selected miRNA which target the RCAN1.4, among molecules included in exosome excreted from NSCLC cell, and investigated the role of the RCAN1.4/targeted miRNAs on tumor growth in vitro, as well as the relationship between RCAN1.4/targeted miRNAs and tumor growth, metastasis, survival and recurrence rate in NSCLC patients.

Materials and Methods

Cell culture

The human NSCLC cell lines A549, H460 and human bronchial epithelial cell line BEAS-2B were cultured in 10% fetal bovine serum (FBS), 100-U/mL penicillin and 100-mg/mL streptomycin (Invitrogen, Carlsbad, CA). Human umbilical vein endothelial cells (HUVECs) were cultured in Medium 200 (Gibco, ON, Canada), supplemented with low serum growth supplement, 5% FBS, 100-U/mL penicillin and 100-mg/mL streptomycin (Gibco, ON, Canada) at 37°C, 95% humidified air, and 5% CO_2. The medium was changed every 2 days and cells at passages 3-5 were used. Cells were purchased from the American Type Culture Collection (ATCC, Manassas, VA, USA).

Clinical specimens

A total of 130 paired samples of human NSCLC and their adjacent noncancerous lung tissues were collected at the time of surgery between 2009 and 2016. Frozen tissue samples were crushed in an achate mortar under liquid nitrogen, homogenized using TissueLyser (Qiagen, Hilden, Germany) in Trizol® reagent (Invitrogen) or RIPA buffer (Millipore, MA, USA). Plasma samples were collected from 48 NSCLC patients and 48 healthy volunteers after informed consent was obtained from individuals. The study was approved by the Institutional Review Board of Asan Medical Center and was conducted in accordance with the International Ethical Guidelines for Biomedical Research Involving Human Subjects.

Exosome isolation

Cell lines (A549, H460 and BEAS-2B) were washed twice with phosphate-buffered saline (PBS) and then grown in serum-free RPMI-1640. After 48 h of incubation, the conditioned medium was collected and centrifuged at 300 g for 10 min, 2,000 g for 10 min, and then 10,000 g for 30 min at 4°C to remove cellular debris thoroughly. The supernatant was centrifuged again at 100,000 g for 70 min at 4°C. The pellets were washed with PBS, and after ultracentrifugation, were re-suspended in PBS. Thawed plasma samples were centrifuged using the same method. Isolated exosomes were quantified using the protein assay (Bio-Rad) and stored at −80°C until needed.

Negative-staining and Immuno-electron microscope

Purified exosomes were fixed in 2% (vol/vol) paraformaldehyde for 5 min at room temperature. After fixation, the 10 ug of exosome suspensions were applied to a formvar/carbon-coated grids (200 mesh) for 3 min and stained with 2% uranyl acetate. After excess uranyl acetate was removed with a filter paper, grids were examined in a transmission electron microscope (EM, Hitachi H7600, Japan) at 80 kV.

Nanoparticle tracking analysis

Exosome size and concentration were analyzed using the NanoSight NS300 system (Malvern Instruments Ltd, Malvern, UK), which allows tracking of the Brownian motion of nanoparticles in a liquid suspension on a particle-by-particle basis. Data were analyzed using the nanoparticle

tracking analysis software (NTA version 2.3 build 0017). To perform the measurements, samples were diluted 10- to 100-fold in PBS to reduce the number of particles in the field of view below 100/frame and readings were taken in triplicate during 60 s at 10 frames per second at room temperature.

Tube forming assay

HUVECs incubated in serum deprivation media for 6 h were seeded at 0.5 x 10^5cells per well in a 12 well plate pre-coated with Matrigel (basement membrane extract: Growth Factor Reduced) (354230, Corning, NY, USA) and incubated in endothelial growth medium containing VEGF or exosomes at 37°C, 95% humidified air, and 5% CO_2. After 3 - 4 h, cells were stained with Calcein AM dye for 10 min at 37°C and were visualized on a Zeiss Observer.Z1 fluorescence microscope system (Carl Zeiss Meditec, Jena, Germany). The total tube lengths of each photograph were measured using Angiogenesis analyzer for image J software.

Wound healing assay

Cell migration was assessed in a wound-healing assay. HUVECs were seeded in each 2 well of Culture-Inserts® (Ibidi, Bonn, Germany) at 2×10^5 cells/well. After incubation for 24 h, each insert was detached and incubated in endothelial growth medium containing exosomes and further cultured until the wound was fully closed at 37°C. Cell migration was ascertained by photography at 10 h using an inverted microscope. The migrated cells to the scraped area were counted. The migrated cells between gaps were normalized to capture of three random sites.

Fluorescence staining and internalization assay

Exosomes were fluorescent stained with CM-DiI (CellTracker, C7000, Molecular ProbesTM, USA) according to the manufacturer's protocol. Briefly, exosomes were re-suspended in DPBS and stained with CM-DiI for 5 min at room temperature, and then for 15 min at 4°C. The labeled exosomes were precipitated again by ultracentrifugation at 100,000 g for 1 h. In addition, HUVEC nuclei were counterstained with DAPI (Molecular Probe Inc. H3570, Oregon, USA). The CM-DiI-labeled exosomes were administered to HUVECs on Confocal Dishes (SPL Life Sciences, 210350, Seoul, Korea) for several times in serum-free conditions. Transported exosomes were visualized on a Zeiss LSM710 confocal system (Carl Zeiss Meditec, Jena, Germany).

miRNA microarray

Accumulating data support that miRNAs are important regulators of angiogenesis. Several miRNAs of them has been found in tumor-derived exosome, stimulating angiogenesis as well as facilitating development of metastasis [33]. Cell line (A549, H460 and BEAS-2B)-derived exosomal RNA including miRNA was extracted using the miRNeasy mini kit (Qiagen, Hilden, Germany) according to the manufacturer's protocol. The miRNA expression profiles of exosomes were established using the Affymetrix GeneChip® miRNA 4.0 Array (Affymetrix, Santa Clara, CA, USA), which is based on miRBase v20 (http://www.mirbase.org). Arrays were prepared, hybridized, and scanned at the local authorized Illumina array service provider (MACROGEN, Seoul, South Korea). All procedures were performed according to the

manufacturer's recommendations. To analyze the differentially expressed miRNAs, quantile normalization was performed to standardize the data across the samples. A549-derived exosome was analyzed against other H460 and BEAS-2B-derived exosomes using a fold-change cut-off of 2.0.

RNA sequencing

HUVECs were treated with cell line (A549, H460 and BEAS-2B)-derived exosomes. After 6 h of incubation, total RNA was extracted from exosome-treated HUVECs using the miRNeasy Mini kit (Qiagen). In order to construct cDNA libraries with the TruSeq RNA library kit, 1 ug of total RNA was used. The protocol consisted of polyA-selected RNA extraction, RNA fragmentation, random hexamer primed reverse transcription and 100nt paired-end sequencing by Illumina HiSeq2500. The libraries were quantified using qPCR according to the qPCR Quantification Protocol Guide and qualified using an Agilent Technologies 2100 Bioanalyzer. The process of RNA Sequencing was performed by a specialized company (Macrogen). Gene-enrichment and functional annotation analysis and pathway analysis for significant gene list were performed based on Gene Ontology (www.geneontology.org/) and KEGG pathway (http://www.genome.jp/kegg/pathway.html).

3′-UTR luciferase reporter constructs and luciferase assays

For validation of RCAN1 targeting by miR-619-5p, RCAN1.4 (NM_203418) 3′-UTR including predicted target sites of miR-619-5p seed sequence were cloned into the pEZX-MT06

Renilla/firefly dual-luciferase reporter plasmid (GeneCopoeia, HmiT004467, Rockville, MD, USA). Mutant constructs were generated with the seed target sites mutated into single (Mut-1:115-121, Mut-2:621-627) or double (Mut-1/2:115-121 and 621-627) site-specific mutation as specified above under the Figure 3. For the RCAN1.4 3′-UTR assay, HUVECs were seeded into 12-well plates one day before transfection, and then co-transfected with 0.8 μg of RCAN1.4 3′-UTR dual-luciferase reporter plasmid (GeneCopoeia) or empty vector, along with 50 nM of miR-619-5p mimic or scrambled miRNA control (miR-control). After 48 h, luciferase activity was measured using the dual-luciferase assay kit (Promega, Madison, WI, USA). Renilla luciferase activity was normalized to firefly luciferase activity. All assays were conducted in triplicate, and each transfection with reporter plasmid was carried out on a different day.

Quantitative real time reverse transcription polymerase chain reaction (qRT-PCR)

Total RNA was extracted using the RNeasy Miniprep kit (Qiagen) according to the manufacturers' protocols. For quantification of mRNA, total RNA was reverse transcribed with High Capacity cDNA Reverse Transcription Kit (Applied Biosystems, Foster City, CA, USA). Quantitative real-time RT-PCR analysis was performed with an ABI 7900 Real-Time PCR System using the SYBR Green Master Mix (Applied Biosystems) with the RCAN1.1 forward 5'-TGGAGCTTCATTGACTGCGA-3', reverse 5'-ACGTCCTAAAGAGGGACTCA-3'; RCAN1.2 forward 5'-GGCGACGTGACTCAGTGTTC-3', reverse 5'-GGTGATGTCCTTGTCATACGTC-3'; RCAN1.4 forward 5'-TTTAGCTCCCTGATTGCCTGT-3', reverse 5'-AAAGGTGATGTCCTTGTCATACG-3'; Beta-actin forward 5'-TTGTTACAGGAAGTCCCTTGCC-3', reverse 5'-

ATGCTATCACCTCCCCTGTGTG-3' primer set according to the manufacturer's protocol. Beta-actin was used as a loading control. For quantification of matured miRNAs, extracted total RNA was polyadenylated with poly(A) Tailing kit (Ambion) and poly(T) adaptor (5'-GCGAGCACAGAATTAATACGACTCACTATAGG(T)12VN-3') prior to reverse transcription. The ABI 7900 Real-Time PCR System enabled SYBR-green based detection and following primers were used: adaptor reverse 5'-GCGAGCACAGAATTAATACGAC-3'; miR-575 forward 5'- GAGCCAGTTGGACAGGAGC-3'; miR-619-5p forward 5'-GCTGGGATTACAGGCATGAGCC-3'; miR-297 forward 5'-ATGTATGTGTGCATGTGCATG-3'; miR-1207-5p forward 5'-TGGCAGGGAGGCTGGGAGGGG-3'; miR-3149 forward 5'-TTTGTATGGATATGTGTGTGTAT-3'; miR-1260b forward 5'-ATCCCACCACTGCCACCAT-3'; miR-4253 forward 5'-AGGGCATGTCCAGGGGGT-3'; miR-4455 forward 5'-AGGGTGTGTGTGTTTTT-3'; miR-4701-3p forward 5'-ATGGGTGATGGGTGTGGTGT-3'; miR-7975 forward 5'-ATCCTAGTCACGGCACCA-3'; miR-1299 forward 5'-TTCTGGAATTCTGTGTGAGGGA-3'; RNU6B forward 5'-CTCGCTTCGGCAGCACA-3'; RNU48 forward 5'-TGATGATGACCCCAGGTAACTCT-3'; let-7a-5p forward 5'-TGAGGTAGTAGGTTGTATAGTT-3'. let-7a-5p was used as a loading control.

Western blot analysis

Cell lysates and exosomes were prepared using EBC lysis buffer (50-mM Tris–HCl [pH 8.0], 120-mM NaCl, 1% Triton X-100, 1-mM EDTA, 1-mM EGTA, 0.3- mM

phenylmethylsulfonylfluoride, 0.2-mM sodium orthovanadate, 0.5% NP-40, and 5-U/mL aprotinin) and lung tissue samples were prepared using RIPA buffer (Millipore) then centrifuged. Proteins were separated using SDS-PAGE and transferred to PVDF membranes (Invitrogen) for Western blot analysis. Membranes were probed using antibodies against DSCR1 (D6694, RCAN1, 1:1000, Sigma-Aldrich, St. Louis, MO, USA) and β-actin (SC47778,1:2000, Santa Cruz Biotechnology, Santa Cruz, CA) as the first antibody; the membranes were then treated with a horseradish peroxidase-conjugated secondary antibody. All membranes were developed using an enhanced chemiluminescence system (Thermo Scientific, Rockford, IL). Densitometric evaluation was performed using image J Software, and normalization was performed using the corresponding controls depending on the specific analysis.

Statistical analysis

Categorical variables were analyzed using Pearson's chi-square test or Fisher's exact test. Continuous variables were analyzed using a Student's *t*-test or ANOVA. Overall survival curves were plotted using the Kaplan-Meier method and were compared using a log-rank test. All tests of significance were two-sided, and differences between groups were considered to be significant when the *P*-value was $< .05$. All statistical analyses were performed with SPSS software version 22.0 (IBM Corp., Armonk, NY).

Results

Exosomes released from A549 cells induce tube formation in HUVECs

To confirm the size of exosomes released from NSCLC cells, we isolated exosomes from cell culture media using ultracentrifugation and examined using the NanoSight LM10. The mean particle diameter was 160 to 190 nm (Fig. 1A; A549, 180.3±1.6 nm; H460, 163.9±4.4 nm; BEAS-2B, 171.2±4.0 nm), so the particles were characterized as exosomes. The size of exosomes also was confirmed by EM (Fig. 1B). Next, we investigated whether exosomes released from NSCLC cells could enhance the angiogenic behavior of endothelial cells *in vitro*. The tube length was increased in HUVECs treated with A549 cell-derived exosomes for 12 h, compared to those treated with H460 and BEAS-2B cell-derived exosomes (Fig. 1C). The migration of HUVECs was significantly enhanced in the presence of A549 and H460 cell-derived exosomes, but not in BEAS-2B cell-derived exosomes (Fig 1D). We also observed that HUVECs take up Dil-labelled exosomes derived from A549 cells in time-dependent manner (Fig. 2). Together, exosomes derived from NSCLC cells stimulated tube formation and migration of endothelial cells and, thus, induced functional reprogramming of endothelial cells *in vitro*.

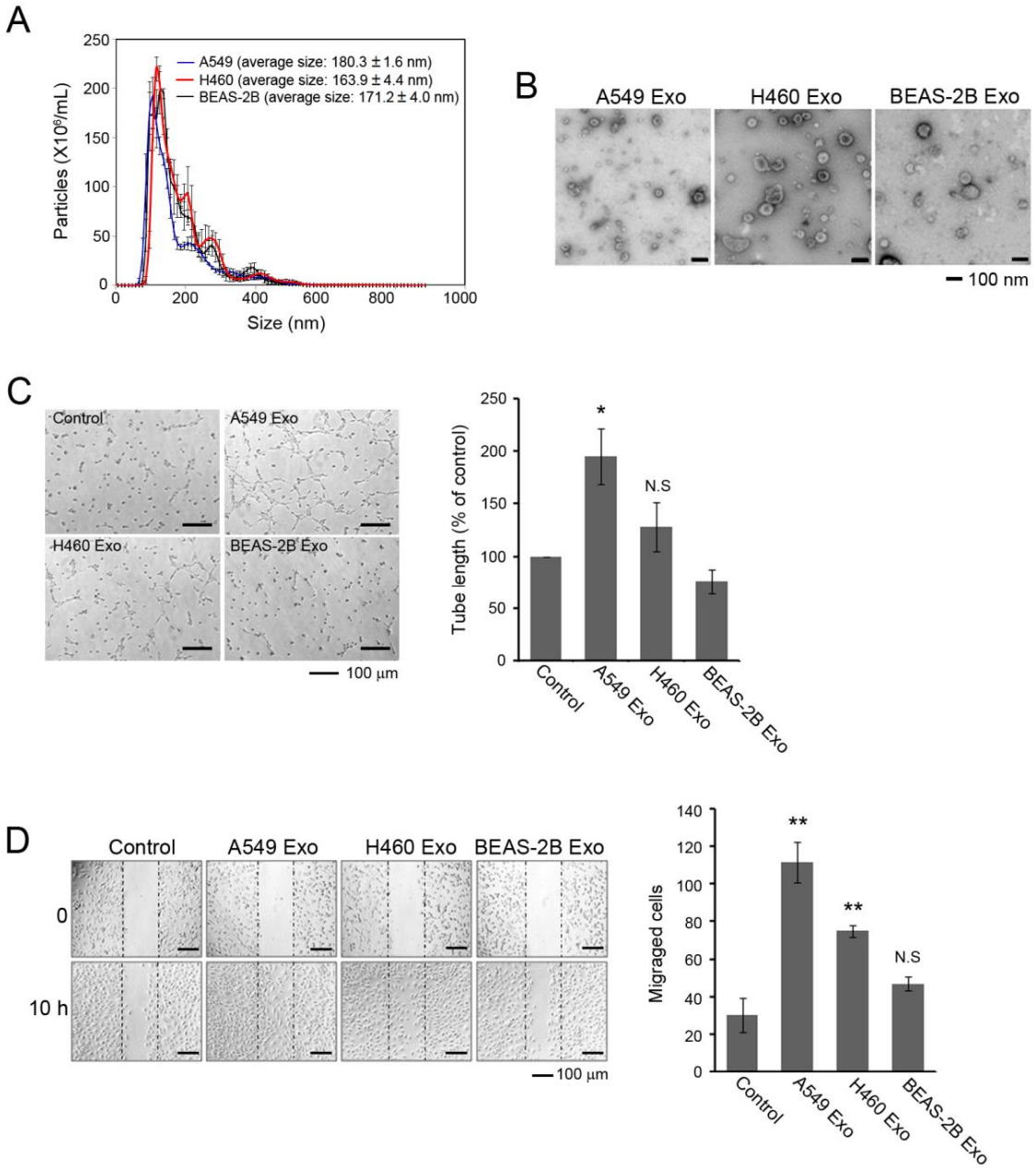

Figure 1. Exosomes released from NSCLC cell-lines effects on tube formation in HUVECs. (A) Nanoparticle tracking analysis of exosomes derived from A549, H460, and BEAS-2B cell-lines. (B) Representative electron micrograph of exosomes. (C) Tube formation assay on HUVECs pretreated with A549, H460 or BEAS-2B cell-derived exosomes. (D) Evaluation of migration of HUVECs treated with A549, H460 or BEAS-2B cell-derived exosomes. All data represent the mean ± standard deviation. *P <0.05, **P <0.005.

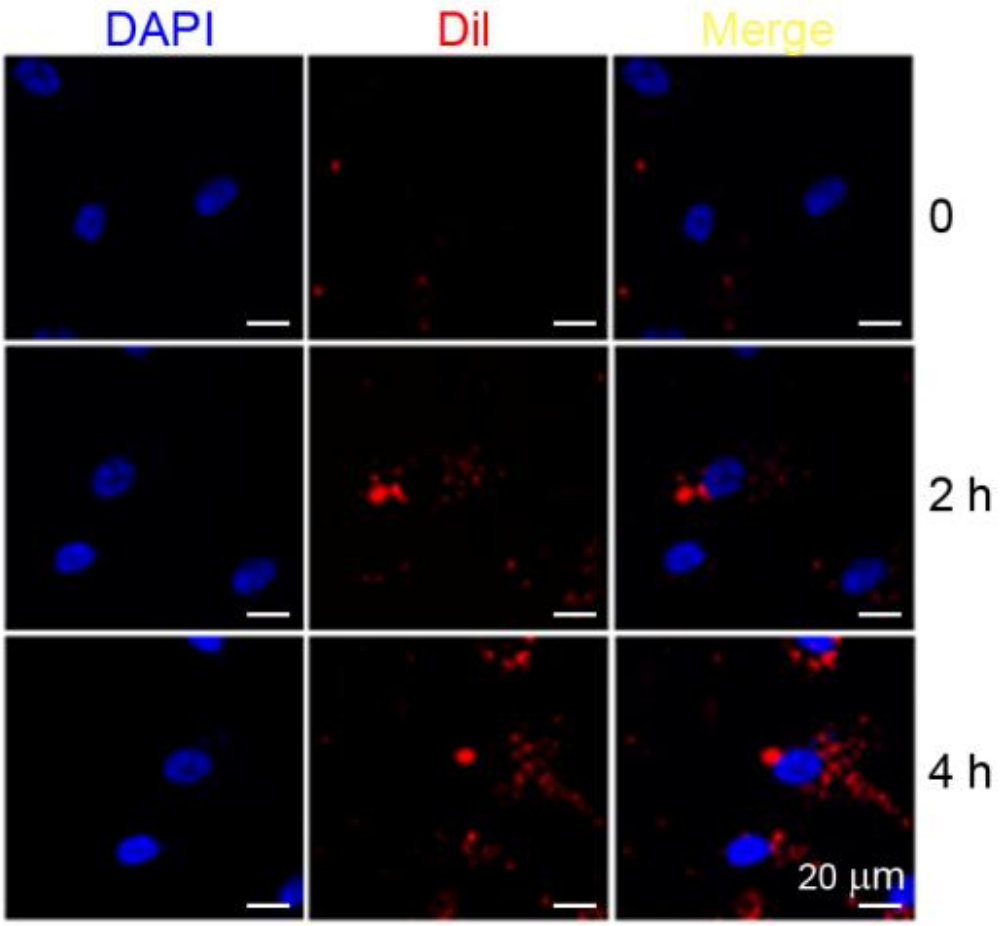

Figure 2. Uptake of exosomes released from A549 cells into endothelial cells. Confocal images of Dil-labelled exosomes taken up by HUVECs. Nucleus and plasma membrane were stained by DAPI and Dil, respectively.

MiRNAs within NSCLC-derived exosome promoted tube formation in HUVECs

We observed the enrichment of short RNAs within NSCLC cell-derived exosome (Fig. 3). Thus, we validated the enriched miRNAs within A549 cell-derived exosome using miRNA assay. We identified 11 upregulated and 2 downregulated miRNAs in A549 cell-derived exosome compared with H460 and BEAS-2B cell-derived exosome (Fig. 4A and B). And then we performed qRT-PCR to avoid false positives of miRNA assay (Figure 5). As a result, we found only miRNAs that were enriched by A549 cell-derived exosome: miRNA-619-5p, miRNA-1260b, miRNA-4253, miRNA-4701-3p and miRNA-1299. The amounts of these miRNAs in exosomes were proportional to the quantity of miRNAs on the cells, although miRNA-619-5p had different pattern (Figure 6). To directly assess the relevance of these miRNAs in tube formation of HUVECs, cells were treated with synthetic miRNA mimics including miRNA-619-5p, miRNA-1260b, miRNA-4253, miRNA-4701-3p and miRNA-1299. As shown in the figure 4C, all miRNAs led to enhancement of tube formation except for miRNA-1299. Thus, specific miRNAs within cancer cell-derived exosome could induce angiogenesis.

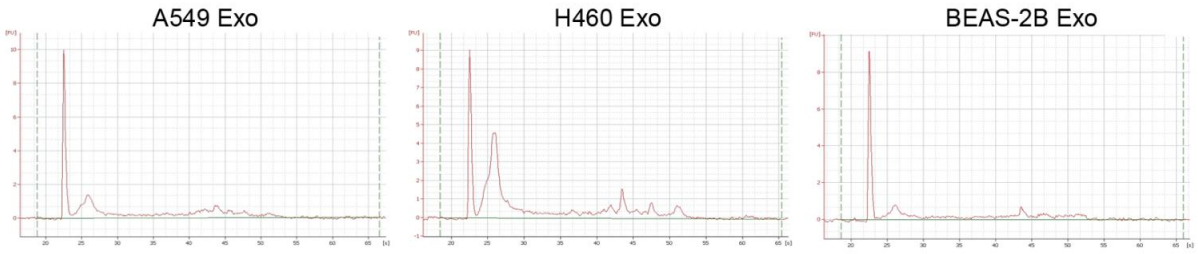

Figure 3. Quantitation and quality of nucleic acid within non-small cell lung cancer cell-derived exosomes.

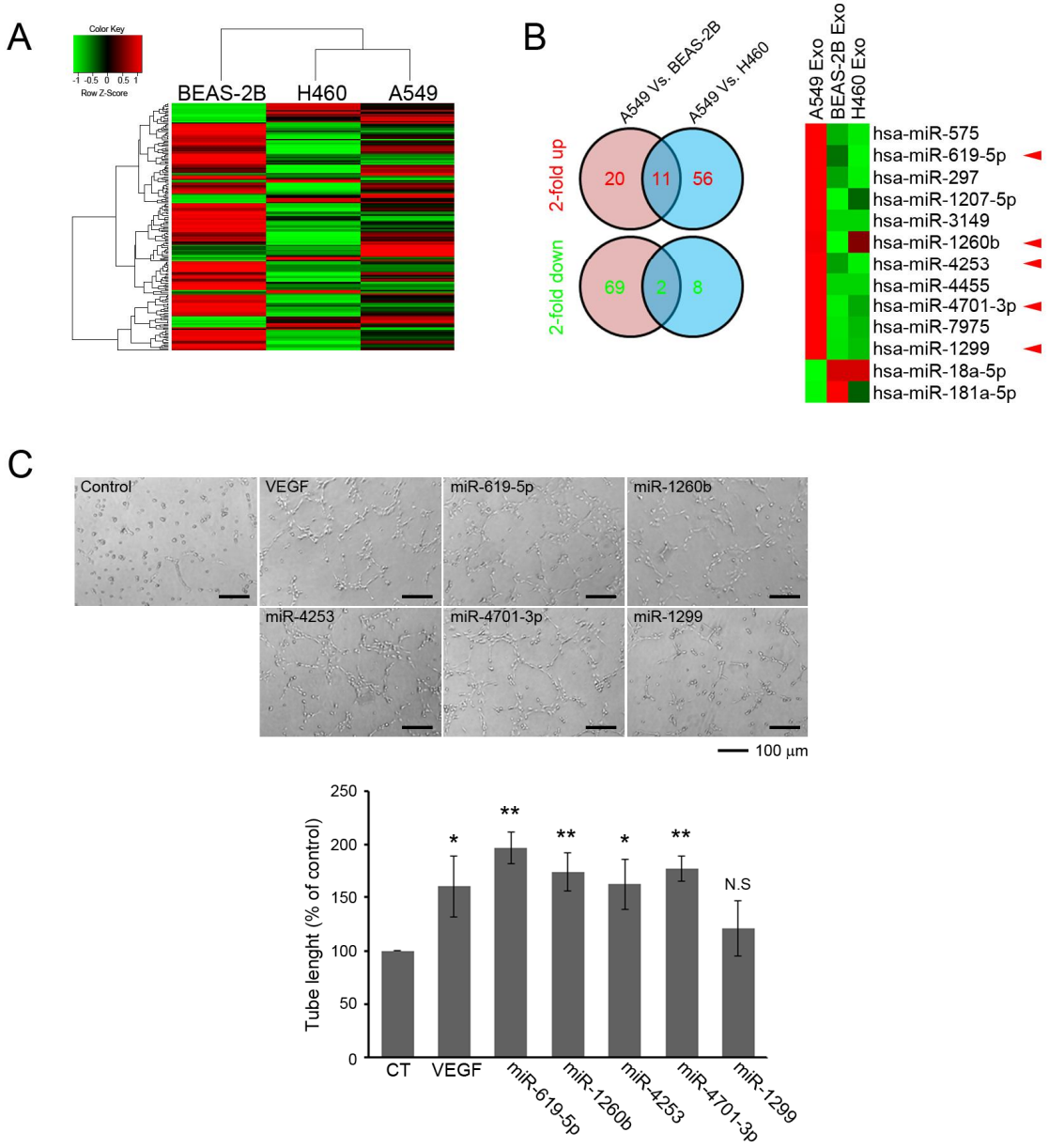

Figure 4. miRNA array in non-small cell lung cancer cell-derived exosome. (A) Unsupervised hierarchical clustering in non-small cell lung cancer cell-derived exosome. (B) Intersection of miRNAs up and down-regulated by A549 cell-derived exosome. (C) Tube formation assay on HUVECs pretreated with the indicated synthetic miRNAs mimics. All data represent the mean ± standard deviation. *P <0.05, **P <0.005. N.S = no significant.

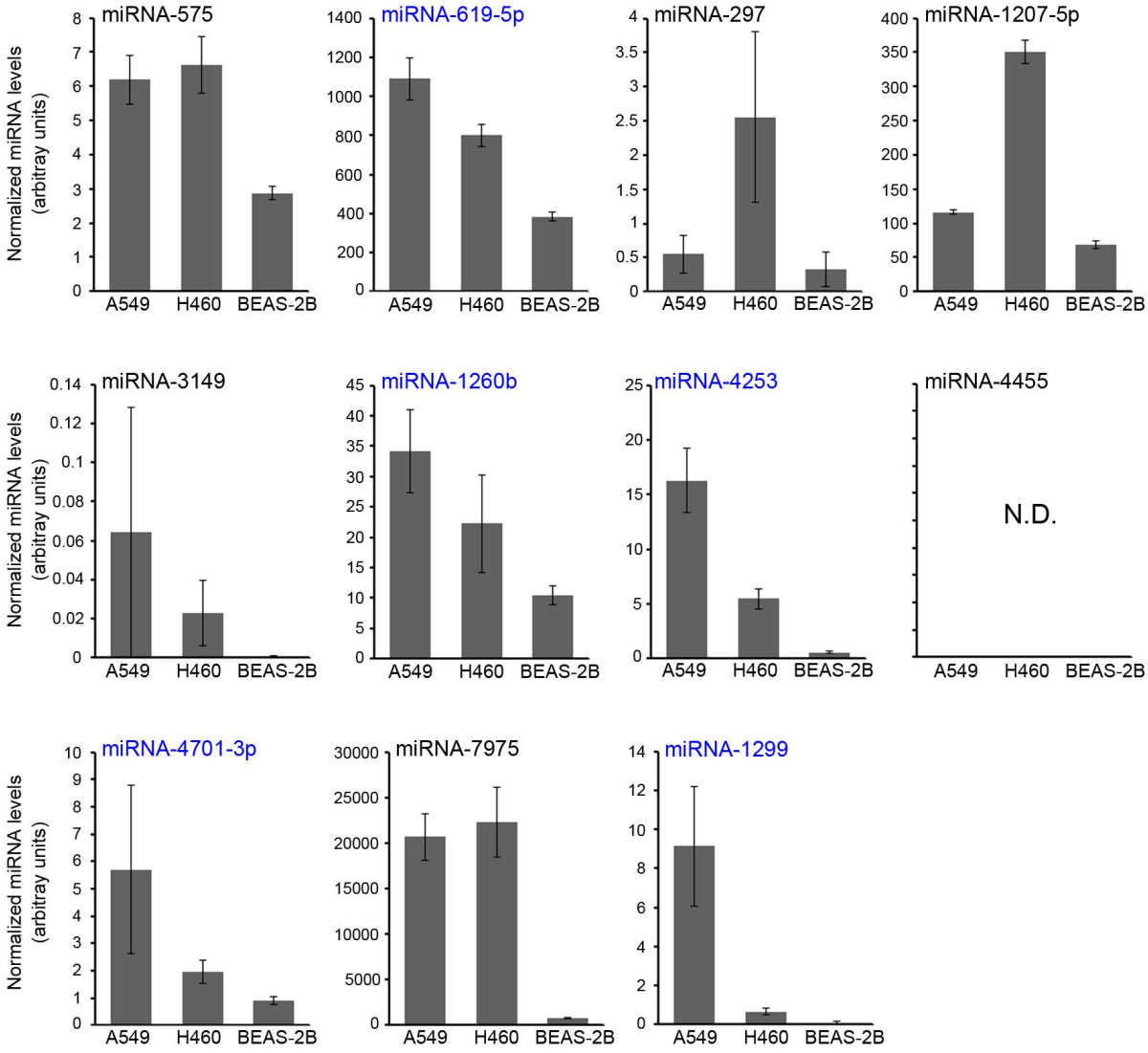

Figure 5. Validation of false positive results in miRNA array. Exosomal miRNAs were determined by RT-PCR. All data represent the mean ± standard deviation.

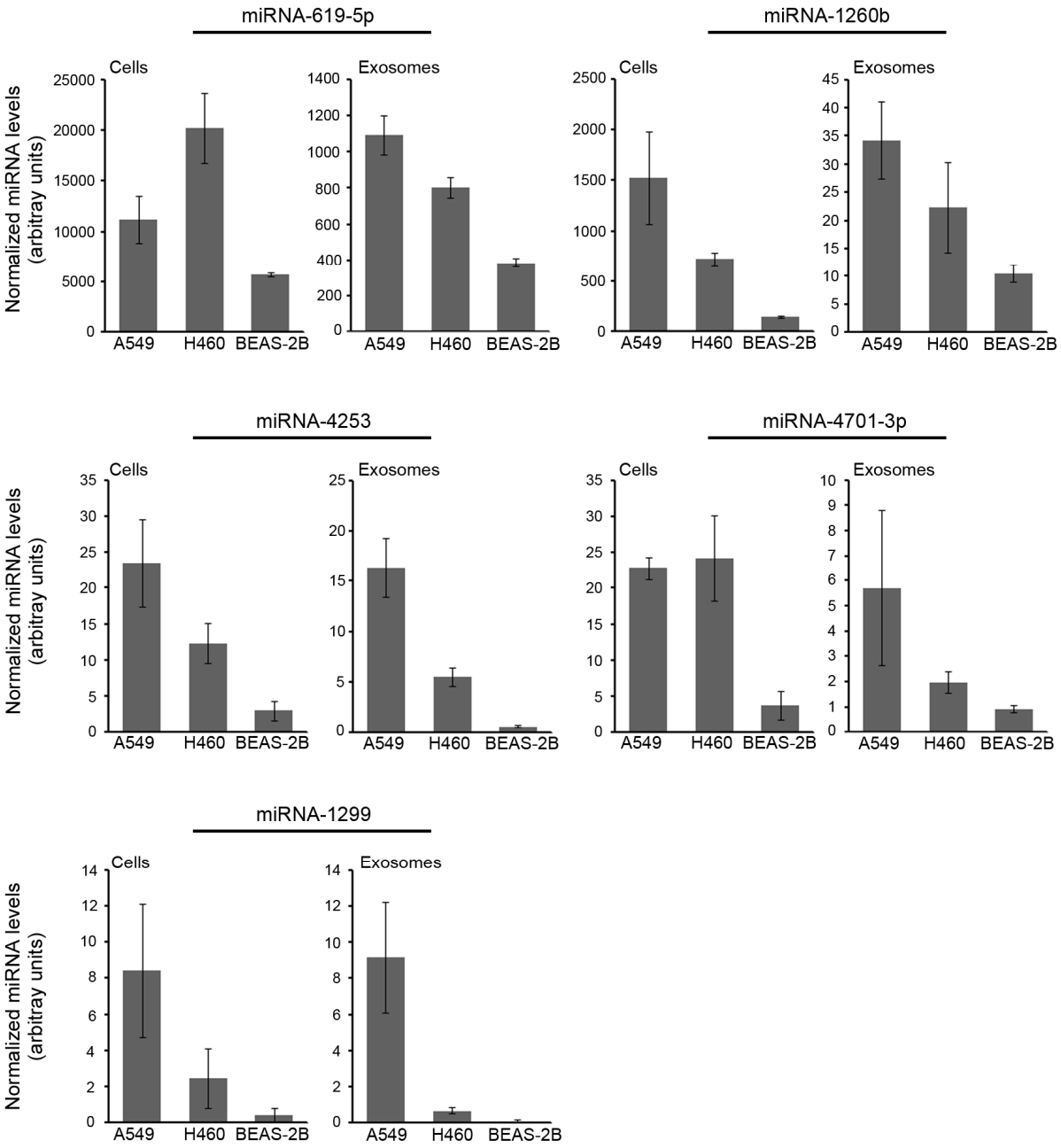

Figure 6. A comparison between cellular miRNAs and exosomal miRNAs. The individual miRNAs were determined by RT-PCR. All data represent the mean ± standard deviation.

Exosomal miRNA-619-5p promoted tube formation by targeting RCAN1.4 in HUVECs

There are miRNAs that can bind to many mRNAs, and one mRNA can be the target of many miRNAs. Because it is difficult to predict how five kinds of miRNAs can target any angiogenesis-related mRNA in endothelial cells, we applied RNA sequencing (RNA-seq) to identify angiogenesis-related mRNA under treatment with individual exosomes. RNA-seq analysis revealed that 16 differentially expressed target genes of which 5 were up-regulated and 11 were down-regulated (Fig. 7A and B). Among of these mRNAs, we focused on mRNA of RCAN1 gene. In addition, we found probable targets of miRNA-619-5p using online algorithms, such as Targetscan. Analysis at miRBase revealed RCAN1.4 to be a potent target of miRNA-619-5p (Fig. 7C). The miRNA-619-5p had two binding sites in 3' UTR of RCAN1.4. To further investigate whether RCAN1.4 was a direct target of miRNA-619-5p, the wild type of target sequence of 3' UTR and the mutant type of target sequence of 3' UTR in RCAN1.4 were cloned into a luciferase reporter vector. HUVECs were then transfected with wild type or mutant type 3' UTR vectors and co-cultured with miRNA-619-5p. A dual-luciferase reporter assay revealed that co-transfection of miRNA-619-5p significantly inhibited the activity of firefly luciferase reporter containing wild type 3' UTR of RCAN1.4. However, this effect was attenuated when the predicted binding sites in 3' UTR were mutated (Fig. 7D). Interestingly, the double mutant type harboring two binding sites in 3' UTR abrogated the effect of miRNA-619-5p completely. Furthermore, treatment with synthetic miRNA-619-5p mimics reduced RCAN1.4 expression, whereas treatment with anti-miRNA-619-5p restored RCAN1.4 expression (Fig. 7E and F, Fig. 8A and B). The other miRNAs including miRNA-1260b, miRNA-4253, miRNA-4701-3p and miRNA-1299 did not target RCAN1.4 (Figure 8C). These results suggest that miRNA-619-5p could target RCAN1.4 through two binding sites in 3' UTR.

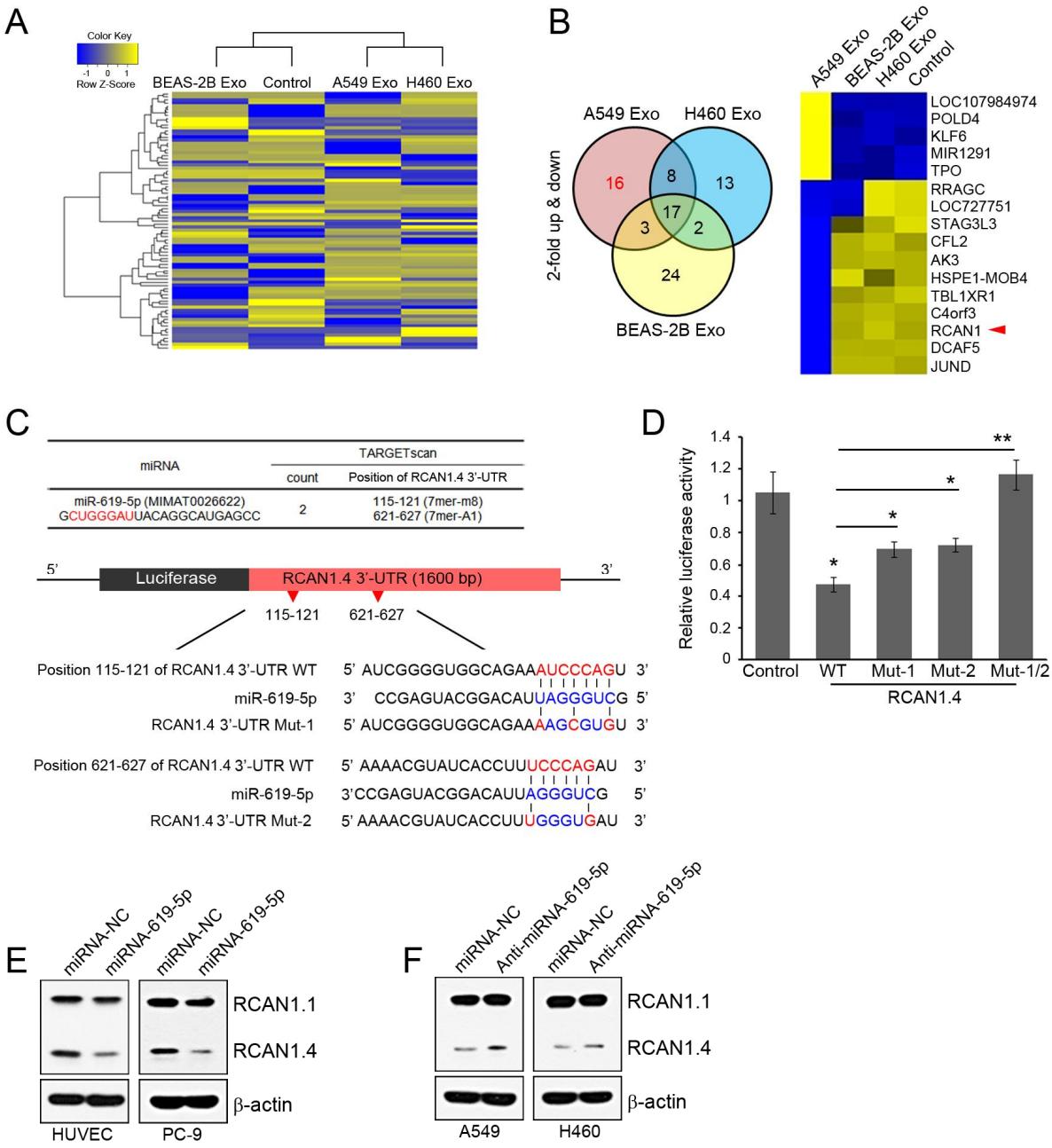

Figure 7. Exosomal miRNA-619-5p targeted RCAN1.4 in endothelial cells. (A) Unsupervised hierarchical clustering in HUVECs after treatment of the indicated exosomes. (B) Intersection of mRNAs up and down-regulated by A549 cell-derived exosome. (C) RCAN1.4 was predicted by Targetscan. Diagram of RCAN1.4 3' UTR containing reporter constructs. (D) Luciferase

reporter assays in HUVECs, with co-transfection of wild type or mutant type RCAN1.4 3' UTR and miRNA-619-5p mimic. The protein levels of RCAN1.4 in HUVECs and non-small cell lung cancer cells after transfection with (E) miRNA-619-5p mimic and (F) anti-miRNA-619-5p. All data represent the mean ± standard deviation. *P <0.05, **P <0.005.

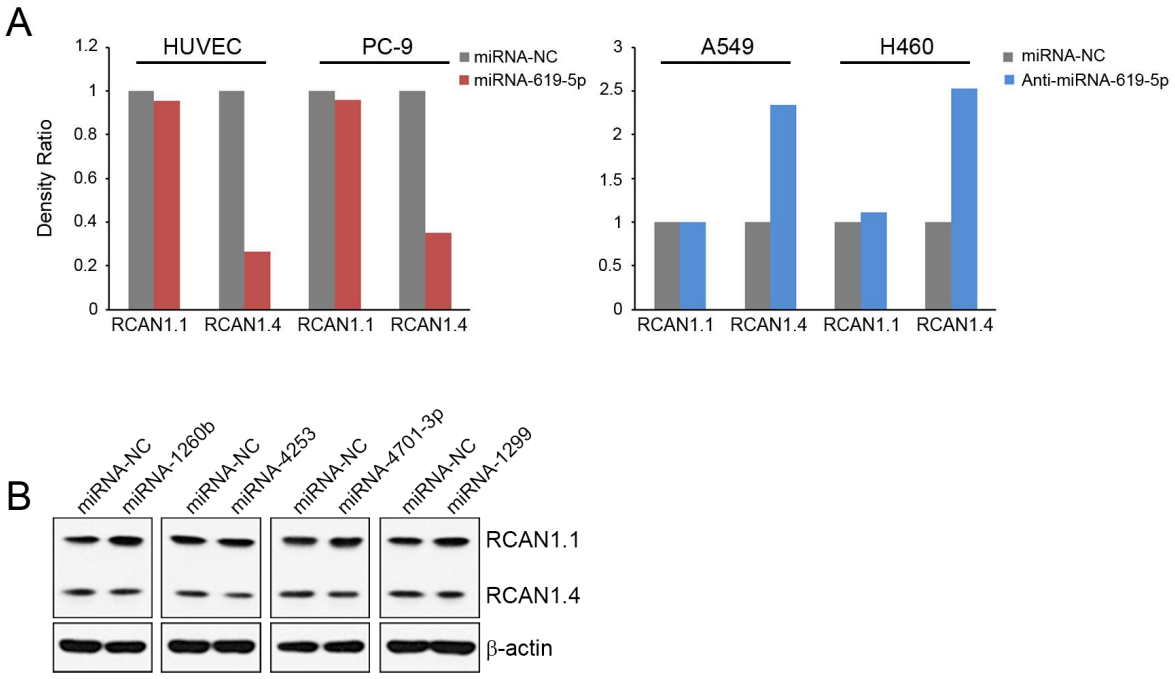

Figure 8. The effect of other miRNAs on RCAN1.4. Densitometric analysis of the protein levels of RCAN1.4 in HUVECs and non-small cell lung cancer cells after transfection with (A) miRNA-619-5p mimic and (B) anti-miRNA-619-5p. (C) The protein levels of RCAN1.4 in HUVECs after transfection with the indicated miRNAs.

RCAN1.4 mRNA levels were associated with survival of patients with NSCLC

We obtained a total of 130 pairs of surgically resected human NSCLC and adjacent noncancer lung tissues. The TNM stages at the time of surgery were as follows: 40 (30.8%) in stage 1, 17 (13.1%) in stage 2, 59 (45.4%) in stage 3 and 14 (10.8%) in stage 4. A total of 43 patients (33.1%) died, showing overall survival duration of 45.9 months. The RCAN1.4 protein and mRNA levels were significantly decreased in lung cancer tissues compared with normal lung tissues (Figure 9A, 9C). These results were consistent when the analyses were performed by dividing into early stage and advanced stage (Figure 9B, 9D). On the contrary, the miRNA-619-5p levels were significantly increased in NSCLC tissues compared with normal lung tissues (Figure 9E, 9F). In addition, the miRNA-619-5p levels were significantly increased in exosomes obtained from NSCLC patients compared with those from healthy volunteers (Figure 9G). We found that there was a significant inverse correlation between the levels of miRNA-619-5p and RCAN1.4 mRNA (Figure 9H, $P = 0.001$). However, the other two transcripts, RCAN1.1 and RCAN1.2 exhibited no significant difference (Figure 10A and B).

Clinical association studies found that RCAN1.4 mRNA levels were significantly associated with overall survival. Kaplan-Meier survival curve showed that patients with low RCAN1.4 mRNA expression levels showed poorer overall survival (41.6±2.7 months) than those with high RCAN1.4 mRNA expression levels (50.3±2.4 months, $P = 0.020$, Figure 11A). However, RCAN1.1 and RCAN1.2 mRNA levels had no significant effect on the overall survival of patients with NSCLC (Figure 11B and C).

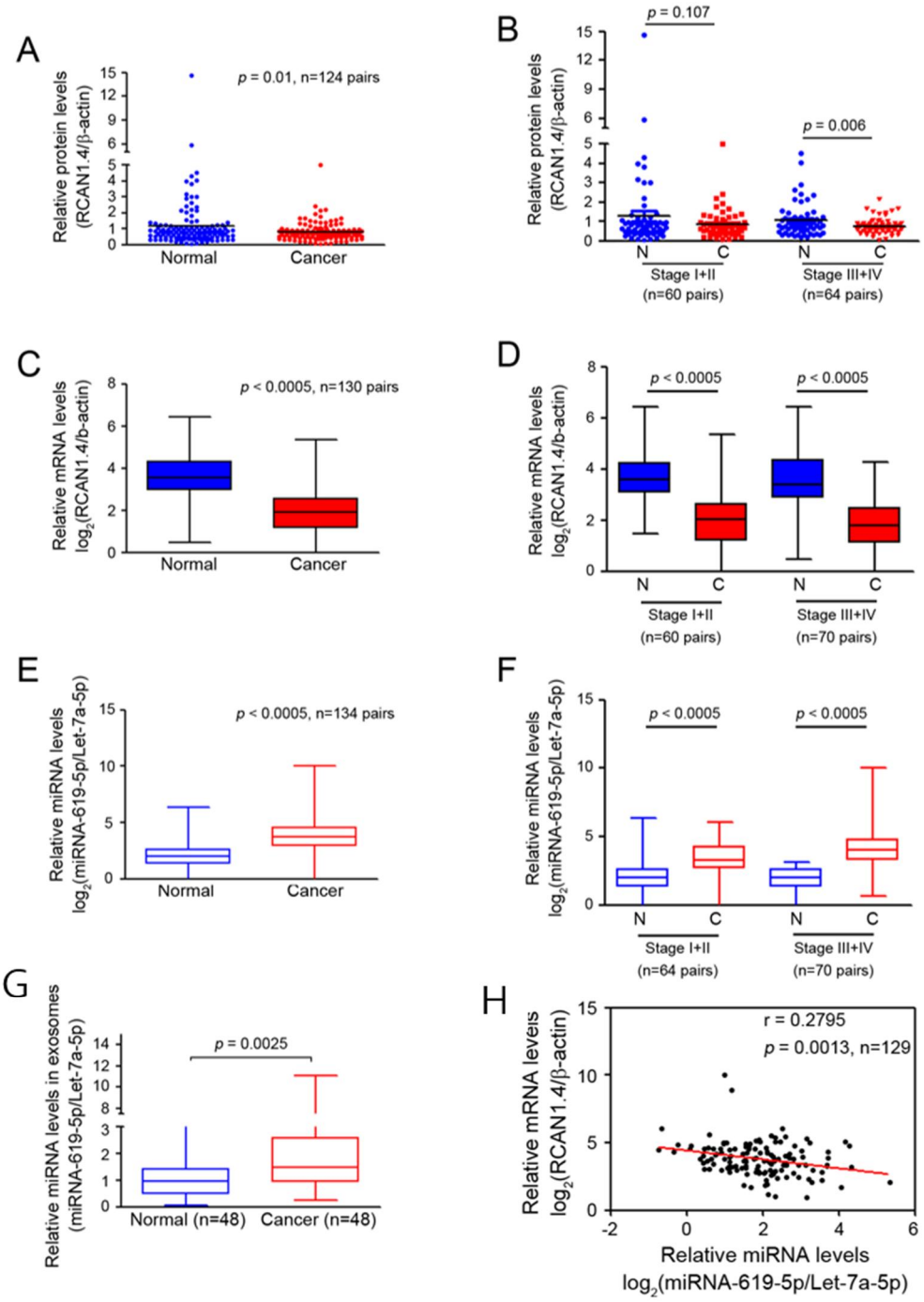

Figure 9. The expression of RCAN1.4 and miRNA-619-5p in patients' tissue with non-small cell lung cancer. (A and B) Scatter plot of RCAN1.4 protein levels in paired lung cancer tissues and adjacent non-cancer lung tissues. (C and D) The mRNA levels of RCAN1.4 transcripts in

130 pairs of non-small cell lung cancer samples. (E and F) Box plots indicate RCAN1.4 mRNA levels in paired non-small cell lung cancer samples. (G) The miRNA-619-5p levels within exosomes from plasma of 48 patients with non-small cell lung cancer and 48 healthy volunteers. (H) The relationship between RCAN1.4 and miRNA-619-5p in lung cancer tissues.

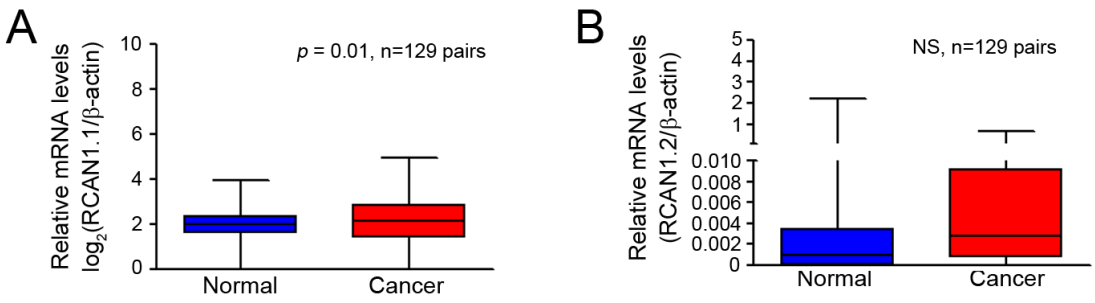

Figure 10. The expression of (A) RCAN1.1 and (B) RCAN1.2 mRNA levels in paired lung cancer tissues and adjacent non-cancer lung tissues.

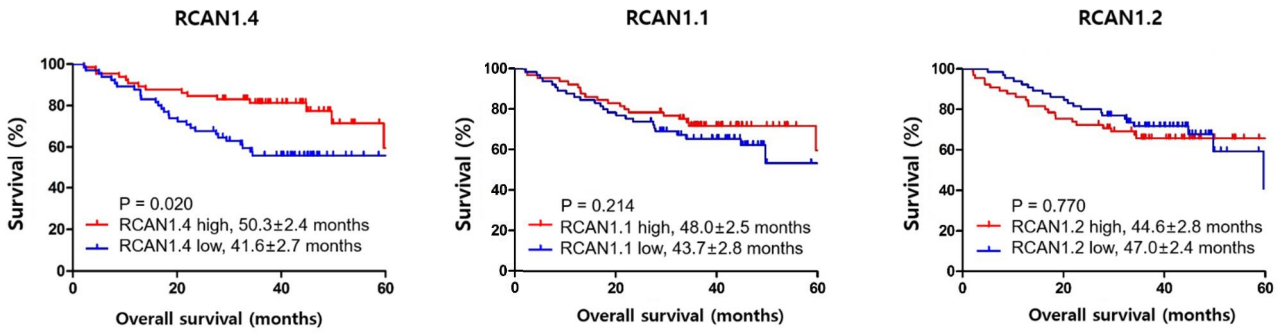

Figure 11. Kaplan-Meier plot of overall survival. (A) Patients with high RCAN1.4 protein levels showed significantly improved survival. These results were not consistent with patients with (B) high RCAN1.1 and (C) RCAN1.2.

Discussion

The present study is the first study to demonstrate that the expression of RCAN1.4 was decreased in NSCLC cell lines and in NSCLC patient's tissues. Clinical analysis indicated that overexpression of RCAN1.4 was associated with improved survival in patients with NSCLC. We found that two binding sites in 3' UTR of RCAN1.4 were the potential targets of miRNA-619-5p. Mutation of these sites attenuated the effect of miRNA-619-5p. Furthermore, treatment with anti-miRNA-619-5p restored RCAN1.4 expression.

Previous studies have confirmed that individuals with Down's syndrome have a reduced incidence of solid tumors compared with the normal population [25]. RCAN1 is located on chromosome 21 and encodes a protein that suppresses VEGF-mediated angiogenic signaling by the calcineurin pathway. Angiogenesis is crucial for tumor development and progression. A previous study showed that the increase in expression afforded by a single extra transgenic copy of RCAN1 was sufficient to confer significant suppression of tumor growth, as a consequence of a deficit in tumor angiogenesis arising from suppression of the calcineurin pathway [25]. Activated calcineurin dephosphorylates multiple residues in the regulatory domain of NFAT, leading to activation of their transcriptional activity. NFATs have been reported to regulate cancer cell invasion, motility and angiogenesis [34]. NFATs are primary transcription activators for the RCAN1.4 gene. As a negative regulator of calcineurin/NFAT pathway, RCAN1.4 has been reported to suppress endothelial cell migration, neovascularization, and tumor growth with reduced vascularity [35, 36]. Irrespective of calcineurin/NFAT pathway, there was a report that the expression level of CnAα, an isoform of calcineurin, might be associated with bone metastasis in patients with small cell lung cancer [30].

However, a calcineurin-independent mechanism may exist in RCAN1.4-mediated tumor suppression. One study noted that RCAN1.4 could interact with Raf-1 kinase and participate in Raf-1-mediated intracellular signaling in HUVECs [37]. In lymphoma cells, RCAN1.4 was shown to interact with IkBa and affect its Y42 phosphorylation, finally inhibiting NF-kB signaling activity [31]. One study demonstrated that NFE2L3 was overexpressed in thyroid cancer and it was functionally important in RCAN1.4–mediated 3D cell growth and invasion [32]. The present study showed the interaction between RCAN1.4 and miRNA-169-5p included exosome excreted from NSCLC cell. We also demonstrated that two binding sites in 3' UTR of RCAN1.4 and anti-miRNA-169-5p mimics could be potential therapeutic target in NSCLC *in vitro*. Although miRNA-169-5p level did not show any relation with survival, the overexpression of RCAN1.4 was associated with significantly improved survival in NSCLC patients in clinical analysis. There might be other mechanisms regarding regulation of RCAN1.4, as well as interaction between RCAN 1.4 and miRNA-169-5p. In addition, the amount of miRNA made in cells might be differed from the amount of miRNA excreted as a form of exosome, resulting in discordant results between *in vitro* and *in vivo*. Lastly, the selection bias might affect the clinical analysis which used surgically obtained tissues, especially in advanced stage which only highly selective patients received surgical resection.

Conclusions

Tumor-derived exosomes may promote tumor growth through the modulation of RCAN1.4, which may be an endogenous tumor suppressor of NSCLC. Therefore, RCAN1.4 and the level of miRNA-619-5p within exosome may be utilized as a diagnostic and prognostic indicator of NSCLC. In addition, RCAN1.4 and miRNA-619-5p may serve as a therapeutic target in patients with NSCLC.

References

1. Little AG, Gay EG, Gaspar LE, Stewart AK. National survey of non-small cell lung cancer in the United States: epidemiology, pathology and patterns of care. Lung cancer 2007;57(3):253–60.
2. Jung KW, Won YJ, Kong HJ, Oh CM, Shin A, Lee JS. Survival of Korean adult cancer patients by stage at diagnosis, 2006-2010: national cancer registry study. Cancer Res Treat. 2013;45(3):162–71.
3. Maemondo M, Inoue A, Kobayashi K et al., Gefitinib or chemotherapy for non–small-cell lung cancer with mutated EGFR. N Engl J Med. 2010;362(25):2380–8.
4. Shaw AT, Kim DW, Nakagawa K, et al., Crizotinib versus chemotherapy in advanced ALK-positive lung cancer. N Engl J Med. 2013;368(25):2385–94.
5. Lötvall J, Hill AF, Hochberg F, et al., Minimal experimental requirements for definition of extracellular vesicles and their functions: a position statement from the International Society for Extracellular Vesicles. J Extracell Vesicles 2014;3:26913.
6. Mittelbrunn M, Sánchez-Madrid F. Intercellular communication: diverse structures for exchange of genetic information. Nat Rev Mol Cell Biol. 2012;13(5):328–35.
7. Boon RA, Vickers KC. Intercellular transport of microRNAs. Arterioscler Thromb Vasc Biol. 2013;33(2):186–92.
8. Valadi H, Ekström K, Bossios A, Sjöstrand M, Lee JJ, Lötvall JO. Exosome-mediated transfer of mRNAs and microRNAs is a novel mechanism of genetic exchange between cells. Nat Cell Biol. 2007;9(6):654–9.
9. Jiang X, Hu S, Liu Q, Qian C, Liu Z, Luo D. Exosomal microRNA remodels the tumor microenvironment. PeerJ. 2017;5:e4196.

10. Kahlert C, Kalluri R. Exosomes in tumor microenvironment influence cancer progression and metastasis. J Mol Med(Berl). 2013;91(4):431–7.

11. Zomer A, Maynard C, Verweij FJ, et al., In vivo imaging reveals extracellular vesicle-mediated phenocopying of metastatic behavior. Cell 2015;161(5):1046–57.

12. Lazar I, Clement E, Dauvillier S, et al., Adipocyte exosomes promote melanoma aggressiveness through fatty acid oxidation: a novel mechanism linking obesity and cancer. Cancer Res. 2016;76(14):4051–7.

13. Hong BS, Cho JH, Kim H, et al., Colorectal cancer cell-derived microvesicles are enriched in cell cycle-related mRNAs that promote proliferation of endothelial cells. BMC Genomics 2009;10:556.

14. Vader P, Breakefield XO, Wood MJ. Extracellular vesicles: emerging targets for cancer therapy. Trends Mol Med. 2014;20(7):385–93.

15. Kosaka N, Iguchi H, Hagiwara K, Yoshioka Y, Takeshita F, Ochiya T. Neutral sphingomyelinase 2 (nSMase2)-dependent exosomal transfer of angiogenic microRNAs regulate cancer cell metastasis. J Biol Chem. 2013;288(15):10849–59.

16. Zitvogel L, Regnault A, Lozier A, et al., Eradication of established murine tumors using a novel cell-free vaccine: dendritic cell-derived exosomes. Nat Med. 1998;4(5):594–600.

17. Valenti R, Huber V, Filipazzi P, et al., Human tumor-released microvesicles promote the differentiation of myeloid cells with transforming growth factor-β–mediated suppressive activity on T lymphocytes. Cancer Res. 2006;66(18):9290–8.

18. Le MT, Hamar P, Guo C, Basar E, Perdigão-Henriques R, Balaj L, Lieberman J. miR-200–containing extracellular vesicles promote breast cancer cell metastasis. J Clin

Invest. 2014;124(12):5109–28.

19. Chen WX, Liu XM, Lv MM, et al., Exosomes from drug-resistant breast cancer cells transmit chemoresistance by a horizontal transfer of microRNAs. PLoS One 2014;9(4):e95240.

20. Stefanius K, Severage K, de Souza Santos M, et al., Cancer cell exosomes can initiate malignant cell transformation. bioRxiv, 2018. https://doi.org/10.1101/360982.

21. Chan B, Greenan G, McKeon F, Ellenberger T. Identification of a peptide fragment of DSCR1 that competitively inhibits calcineurin activity in vitro and in vivo. Proc Natl Acad Sci U S A. 2005;102(37):13075–80.

22. Lin H, Michtalik HJ, Zhang S, et al., Oxidative and calcium stress regulate DSCR1 (Adapt78/MCIP1) protein. Free Radic Biol Med. 2003;35(5):528–39.

23. van Rooij E, Doevendans PA, Crijns HJ, et al., MCIP1 overexpression suppresses left ventricular remodeling and sustains cardiac function after myocardial infarction. Circ Res. 2004;94(3): e18–26.

24. Hesser BA, Liang XH, Camenisch G, et al., Down syndrome critical region protein 1 (DSCR1), a novel VEGF target gene that regulates expression of inflammatory markers on activated endothelial cells. Blood 2004;104(1):149–58.

25. Baek KH, Zaslavsky A, Lynch RC, et al., Down's syndrome suppression of tumour growth and the role of the calcineurin inhibitor DSCR1. Nature 2009;459(7250):1126–30.

26. Ryeom S, Baek KH, Rioth MJ, et al., Targeted deletion of the calcineurin inhibitor DSCR1 suppresses tumor growth. Cancer Cell 2008;13(5):420–31.

27. Espinosa AV, Shinohara M, Porchia LM, Chung YJ, McCarty S, Saji M, Ringel MD.

Regulator of calcineurin 1 modulates cancer cell migration in vitro. Clin Exp Metastasis 2009;26(6):517–26.

28. Jang C, Lim JH, Park CW, Cho YJ. Regulator of Calcineurin 1 Isoform 4 (RCAN1.4) Is Overexpressed in the Glomeruli of Diabetic Mice. Korean J Physiol Pharmacol. 2011;15(5):299–305.

29. Jin H, Wang C, Jin G, et al., Regulator of calcineurin 1 gene isoform 4, down-regulated in hepatocellular carcinoma, prevents proliferation, migration, and invasive activity of cancer cells and metastasis of orthotopic tumors by inhibiting nuclear translocation of NFAT1. Gastroenterology 2017;153(3):799–811.

30. Ma N, Shen W, Pang H, Zhang N, Shi H, Wang J, Zhang H. The effect of RCAN1 on the biological behaviors of small cell lung cancer. Tumour Biol. 2017;39(6):1010428317700405.

31. Liu C, Zheng L, Wang H, Ran X, Liu H, Sun X. The RCAN1 inhibits NF-kappaB and suppresses lymphoma growth in mice. Cell Death Dis. 2015;6:e1929.

32. Wang C, Saji M, Justiniano SE, et al., RCAN1-4 is a thyroid cancer growth and metastasis suppressor. JCI Insight 2017;2(5):e90651.

33. Zhang J, Li S, Li L, Li M, Guo C, Yao J, Mi S. Exosome and exosomal microRNA: trafficking, sorting, and function. Genomics Proteomics Bioinformatics 2015;13(1):17–24.

34. Mancini M, Toker A. NFAT proteins: emerging roles in cancer progression. Nat Rev Cancer 2009;9(11):810–20.

35. Minami T, Horiuchi K, Miura M, et al., Vascular endothelial growth factor-and thrombin-induced termination factor, Down syndrome critical region-1, attenuates

endothelial cell proliferation and angiogenesis. J Biol Chem. 2004;279(48):50537–54.

36. Iizuka M, Abe M, Shiiba K, Sasaki I, Sato Y. Down syndrome candidate region 1, a downstream target of VEGF, participa tes in endothelial cell migration and angiogenesis. J Vasc Res. 2004;41(4):334–44.

37. Cho YJ, Abe M, Kim SY, Sato Y. Raf-1 is a binding partner of DSCR1. Arch Biochem Biophys. 2005;439(1):121–8.

영문요약

Intercellular communication between cells and their microenvironment is important for tumor growth. Exosomes are released from almost all cell types, including tumor cells. Tumor-derived exosomes have recently received a great deal of attention because of their ability to induce an aggressive phenotype, immune escape, angiogenesis and drug resistance through the horizontal transfer of cellular macromolecules between cancer cells. Here we showed that the only of A549 cell-released exosomes promote an angiogenic phenotype in HUVECs compared to other lung cancer cell-released exosomes. Using a miRNA array approach, we identified that specific miRNAs can modulate angiogenesis in A549 cell-released exosomes. Among these miRNAs, miRNA-619-5p significantly induced angiogenesis in HUVECs. We found that miRNA-619-5p directly targeted RCAN1.4 and ectopic expression of miRNA-619-5p markedly decreased RCAN1.4 expression. In patients with non-small cell lung cancer (NSCLC), the level of RCAN1.4 was significantly lower in cancer tissues than normal lung tissues, whereas the level of miRNA-619-5p was a significantly higher in cancer tissues than normal lung tissues. We also found that there was a significant inverse correlation between the expression of miRNA-619-5p and that of RCAN1.4. In addition, miRNA-619-5p expression was higher in exosomes isolated from plasma of patients with NSCLC than normal. The level of RCAN1.4 was associated with survival of patients with NSCLC. Thus, it might be possible for the level of miRNA-619-5p within exosome to be a utilized as a diagnosis and prognostic indicator for NSCLC patients. We are searching for the detailed mechanisms of angiogenesis and tumor growth through the modulation of RCAN1.4.